

A Review of WBG and Si Devices Hybrid Applications*

Li Zhang*, Zhongshu Zheng and Xiutao Lou

(College of Energy and Electrical Engineering, Hohai University, Nanjing 211100, China)

Abstract: In recent years, next-generation power semiconductor devices, represented by silicon carbide (SiC) and gallium nitride (GaN), have gradually emerged. Because wide-bandgap (WBG) devices have better electrical characteristics than those of silicon (Si) based devices, they have attracted increased attention both from academic researchers and industrial engineers. Employing WBG devices will further improve the efficiency and power density of power converters. However, the current price of WBG devices remains extremely high. Thus, some researches have focused on the hybrid utilization of WBG devices and Si-based devices to achieve a tradeoff between the performance and cost. To summarize the current research on WBG/Si hybrid applications, the issues mentioned above with representative research approaches, results, and characteristics, are systematically reviewed. Finally, the current research on WBG/Si hybrid applications and their future trends are discussed.

Keywords: Silicon carbide (SiC) devices, gallium nitride (GaN) devices, silicon (Si) devices, hybrid application

1 Introduction

Power converters have been widely used in wind and photovoltaic (PV) power generations, multi-electric aircraft, electric transmission, and hybrid electric vehicles^[1-5]. A high efficiency, high power density, and low cost are always the primary requirements of power converters^[6-8].

Increasing the switching frequency is a simple approach for improving the performance of power converters, which can significantly reduce the volume and weight of the filters and increase the power density^[9-13]. However, a high power density based on silicon (Si) devices is difficult to achieve by increasing the switching frequency because the performance of Si devices has reached their theoretical limitations^[14-17]. In recent years, power converters based on Si devices have undergone remarkable upgrades with the usage of WBG devices, such as silicon carbide (SiC) and Gallium nitride (GaN)^[18-20], resulting in an increased junction operating temperature and

higher switching speed capability^[21]. Several full-SiC T-Type inverters were proposed for high-efficiency PV grid-tied applications^[22-24]. Owing to the high switching speed capability of SiC devices, a high power density is achieved in these PV inverters. In addition, a full-SiC two-level inverter with an LCL filter was proposed for aerospace and more electric aircraft applications, which also shows an excellent performance in terms of efficiency and power density. In addition, Liu et al.^[25] employed a GaN high electron mobility transistor (HEMT) into a 6.6 kW on-board vehicle charger, and the efficiency of the entire power stage reaches up to 98.5%.

However, three-level (3L) T-type inverters based on SiC, GaN, and Si devices were developed and compared^[26], and the efficiencies of GaN- and SiC-based converters are up to 98.7% and 98%, respectively. However, the efficiency of a full-Si converter is only 97% (both of which were tested under 2 kW of output power and a 32 kHz switching frequency), which illustrates the superiority of the WBG-based power converters^[27-32]. Nevertheless, the high prices of these WBG devices (both SiC and GaN devices) are still a significant issue preventing them from becoming commercially available. The

Manuscript received August 6, 2020; revised November 27, 2020; accepted January 6, 2021. Date of publication June 30, 2021; date of current version June 3, 2021.

* Corresponding Author, E-mail: zhanglinuaa@hhu.edu.cn

* Supported by the National Natural Science Foundation of China(51677054) and the 16th Six Talent Peaks Project in Jiangsu Province (2019-TD-XNY-001).

Digital Object Identifier: 10.23919/CJEE.2021.000012

price of SiC MOSFET is 8-times that of Si IGBT under a higher current rating, which leads to the high cost of full-WBG power converters. Therefore, compared with full-WBG power converters, the hybrid utilization of WBG/Si devices is an alternative way to achieve the tradeoff between cost and performance.

A hybrid switch with a main high-current Si IGBT and auxiliary low-current SiC MOSFET connected in parallel was proposed^[33], which lowers the cost and overcomes the trailing current issues of Si IGBT. Moreover, a hybrid switch made up of two surface mount technologies (SMTs) based GaN HEMTs and a Si MOSFET was proposed^[34], the high performance of which is achieved by combining the high switching speed capability of the GaN HEMTs and the low conduction resistance of the Si MOSFET. The hybrid application of WBG and Si is not only based on the devices but also based on the circuit topologies. A three-level (3L) active-neutral-point-clamped (ANPC) inverter combined with four SiC MOSFETs and two Si IGBTs has also been proposed^[35]. The maximum efficiency of the 4-SiC 3L-ANPC inverter can reach 99% with 20 kHz switching frequency, which is higher than the full-Si type inverter. Similarly, a 3L-ANPC rectifier based on the hybrid utilization of SiC MOSFETs and Si active switches was proposed^[36], in which all high-frequency switching events are moved to the SiC devices by employing a dedicated modulation scheme, which helps decrease the switching losses. The maximum 99% efficiency at a 45 kHz switching frequency demonstrates the advantages of the hybrid utilization of WBG/Si devices.

In summary, there are three ideas used to achieve the hybrid utilization of WBG/Si devices, i.e., a device level hybrid utilization scheme, a modular level hybrid utilization scheme, and a circuit level utilization scheme. Among them, the device and circuit levels are currently the research hotspots of WBG/Si hybrid applications. In this study, the hybrid applications of WBG and Si devices are reviewed, and the future research prospects are discussed. The

rest of this paper is organized as follows: Section 2 discusses the development experience of power electronics devices and makes a comparative analysis of Si- and WBG-based devices. Sections 3 and 4 respectively summarize the device and modular level, and the hybrid circuit-level utilization schemes, respectively. The principle of the hybrid scheme is described, and some concluding remarks are provided in Section 5.

2 Comparison of Si and WBG devices

As an indispensable aspect of power electronics devices, innovations into power semiconductor devices and semiconductor technology have allowed the entire power electronics industry to flourish. As shown in Fig. 1, the development of power semiconductor devices has gone through four critical stages^[1-4]. Since the invention of the thyristor in the 1950s, semiconductor devices based on Si materials have occupied a dominant position in power electronic devices owing to their important material resources, low production cost, and simple manufacturing process. Then, in the mid-1970s, with the development and application of full-controlled devices, such as a gate turn-off thyristor(GTO), giant transistor(GTR), and power MOSFET, power electronics technology entered a new stage. In the 1980s, with the appearance of MOS IGBT and the commercialization of the power MOSFET, the development of power semiconductor devices began, which attracted increased attention, and such devices were applied to many different fields. Although MOSFET has apparent advantages in terms of high-frequency applications, its on-state resistance increases rapidly with the increase in the blocking voltage, and thus it is mostly used in medium and low voltage applications^[37-39]. IGBT has a low voltage drop and fast switching speed and is widely used in medium frequency and high-power applications. At the turn of this century, with the commercialization of SiC diodes, WBG devices represented by SiC and GaN began attracting attention, which also lead a re-innovation of power electronics technology.

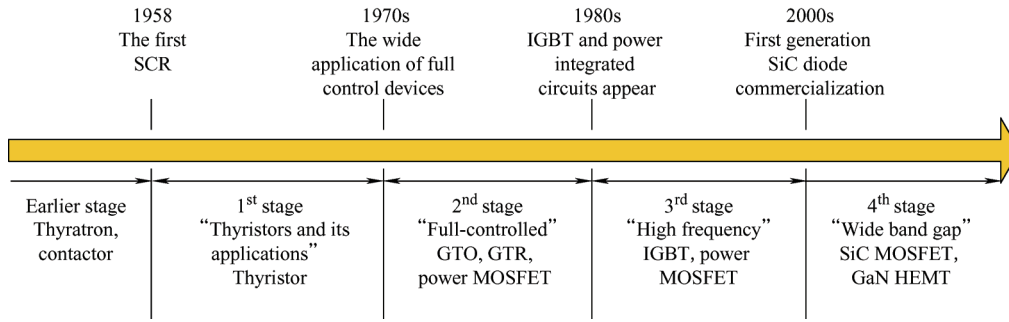


Fig. 1 Development of power devices

At present, the application of Si-based power devices has been fully developed. However, Si-based power devices cannot be employed when the voltage is higher than 6.5 kV, the current is higher than 2 kA, or the temperature is higher than 250 °C^[40]. By contrast, WBG devices, as represented by SiC and GaN devices, have more advantages in these aspects owing to their material properties. The characteristics of these three materials are compared^[41], as shown in Fig. 2. It can be seen that the energy gap width of a WBG material is 3-times that of Si material. Therefore, the power semiconductor device based on the WBG material can withstand a higher temperature. The critical breakdown field of the WBG material is approximately 10-times that of Si material. Thus, power semiconductor devices based on WBG material have a higher breakdown voltage. In general, the conduction loss is inversely proportional to its breakdown field strength. Therefore, at the same power level, the power semiconductor device based on a WBG material has a lower conduction loss and little temperature dependence. The electron saturation drift speed of the WBG material is about twice that of Si material, and thus power semiconductor devices based on a WBG material can operate at higher switching frequencies^[40-45].

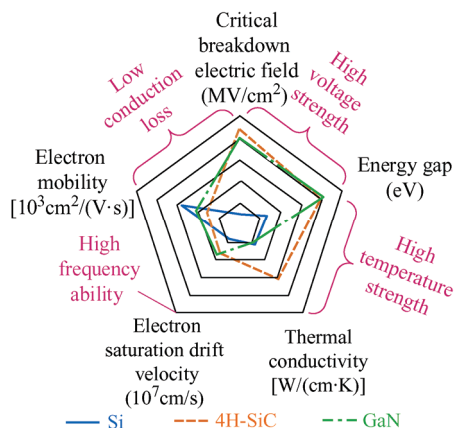


Fig. 2 Comparison of semiconductor material properties

According to the above advantages, WBG-based power semiconductor devices are more suitable for high-frequency and high-power applications.

Fig. 3 shows the limitation of the commonly used semiconductor power devices. It can be concluded that Si-based power semiconductor devices have significant limitations in high-frequency and high-power conditions. Owing to a high breakdown voltage, the ability to withstand a high temperature, fast switching speed, and low conduction loss, WBG devices are the key to improving the efficiency and power density of power converters in the future^[46-47].

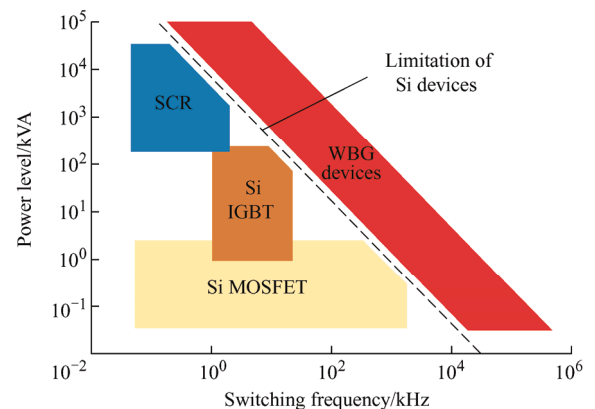


Fig. 3 Operating limits of commonly used semiconductor power devices

The advantages of power semiconductors based on WBG materials are remarkable. However, owing to their complex manufacturing processes and production difficulties, the overall price of existing commercial products is still relatively high. Fig. 4 shows the cost curves of Si MOSFET, Si IGBT, and SiC MOSFET with a partial rated voltage of 650 V and TO-247 packages at different current levels, according to the price listed on the official website of Digikey (<http://www.digikey.com/>). It can be seen that the cost of SiC MOSFETs is much higher than that of Si

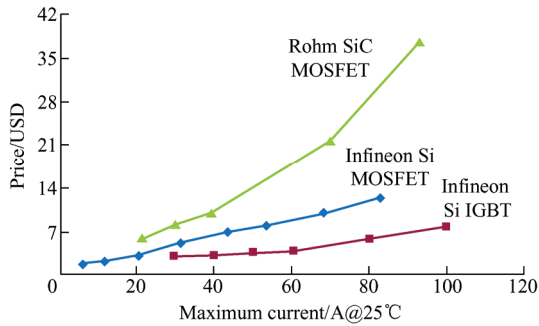


Fig. 4 Diagram of different prices of switch devices

devices at a higher current, which is approximately 2-4 times that of Si MOSFETs and 4-6 times that of Si IGBTs.

WBG devices have not been widely used in industrial applications owing to their high prices and manufacturing process limitations, and WBG devices cannot be commonly used in various power supply devices. However, owing to their high breakdown voltage, ability to withstand high temperatures, fast switching speed, low conduction loss, and other advantages, WBG devices have significant benefits in improving the converter efficiency and power density. Therefore, studies on the hybrid applications of WBG and Si devices are highly significant.

3 Overview of device and modular level applications

From the perspective of significantly reducing the switching losses, WBG power devices such as SiC and GaN devices achieve a superior performance over Si devices. However, the current market price of WBG devices is much higher than that of Si devices, which limits its widespread use, particularly in high-power applications owing to the large number of switching devices used. By contrast, the current commercial WBG power devices are only available at a small current level, which limits the direct replacement of the Si IGBT with WBG devices^[1]. It is also impractical to replace a single Si IGBT with multiple WBG devices in parallel at a high current owing to the complexity of the control and the uncertainty^[48].

Paralleling semiconductor power devices is an effective way to realize a higher rated current in power conversion systems^[49-50]. A hybrid switch (HyS) composed of different devices applied in parallel can fully utilize their respective advantages. A Si/WBG

HyS has been verified to achieve a high efficiency and is a cost-effective switching device for high-voltage and high-power applications^[51].

3.1 Device-level application

3.1.1 Si device + SiC Schottky barrier diode (SBD)

A SiC SBD is the first SiC device used in commercial applications. Owing to its excellent reverse recovery characteristic, SiC SBD is widely used in various power converters. As a fast recovery diode, Si may indeed be reaching its limits from the perspectives of loss reduction and improved efficiency. A simple method is to replace a fast recovery Si diode with SiC SBD and connect the Si IGBT or Si MOSFET in an anti-parallel manner^[52-53], as shown in Fig. 5.

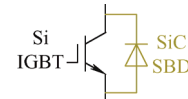


Fig. 5 Si IGBT + SiC SBD HyS

The switching characteristics of Si IGBT+SiC SBD HyS were previously tested^[54]. The results show that turn-on energy losses of Si IGBT are reduced by 55%, and that the reverse recovery loss of SiC SBD can be basically reduced. A 3L topology with anti-parallel diodes partially replaced by SiC SBDs, in which the switching losses were reduced by 10% at the rating power, was proposed^[52].

The static and dynamic characteristics of SiC SBD and a fast recovery Si diode were compared and analyzed elsewhere^[55-56]. The results demonstrate that the total switching loss and EMI level generated by SiC SBD are lower than that of a fast recovery Si diode. The HyS composed of SiC SBD and Si IGBT can achieve a higher efficiency, improve the Si IGBT reliability, and reduce the heatsink volume^[56].

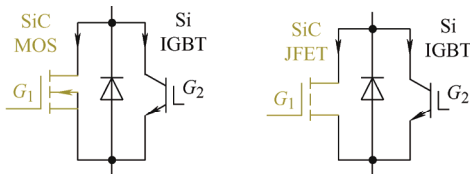
3.1.2 Si IGBT + SiC MOSFET/JFET

Compared with Si IGBT, SiC MOSFET has a superior switching performance owing to its inherent material properties. A major issue of SiC MOSFETs is a high conduction loss under a large current^[51, 57-58]. In addition, it is currently difficult to develop a low-cost SiC MOSFET with a high current rating. By contrast, Si IGBT is well known for its low conducting voltage

drop under a large current owing to the conductivity modulation effect. However, the slow switching characteristic of an IGBT prevents it from operating at a high frequency. Owing to the trailing current, the turn-off loss is also high^[59].

Thus, it is natural to propose a HyS by combining one Si IGBT and one SiC MOSFET in parallel, which fully integrate the low conduction loss of a Si IGBT and the low switching loss of a SiC MOSFET, as shown in Fig. 6a. Because of the similarity between Si IGBT+SiC MOSFET HyS and Si IGBT+SiC JFET HyS^[51], only Si IGBT + SiC MOSFET HyS is analyzed in this article. Detailed introductions of Si IGBT + SiC JFET HyS are presented elsewhere^[60-61]. Research on Si IGBT+SiC MOSFET HyS mainly focuses on the following aspects.

The first aspect is the SiC/Si current ratio of HyS. To lower the cost of HyS, it is recommended to use a low-current SiC MOSFET and a high-current Si IGBT^[57, 62]. The SiC/Si current ratio is less than 1. A 1:1 SiC/Si current ratio of HyS was previously introduced in detail^[63-64]. A SiC/Si current ratio of 1:4 has also been proposed^[58]. Moreover, a SiC/Si current ratio of 1:5 has been reported^[59]. It is clear that the lower SiC/Si current ratio is, the lower the cost requirement. However, the SiC/Si current ratio should be limited by consideration of the safe operating area (SOA) of the SiC MOSFET^[51]. To optimize the SiC/Si current ratio, a peak junction temperature algorithm for HyS has been introduced^[48].



(a) Si IGBT+SiC MOSFET HyS (b) Si IGBT+SiC JFET HyS
Fig. 6 Two types of HyS

The second aspect is the on-state and switching characteristics of HyS. The static I - V characteristics of Si IGBT, SiC MOSFET, and SiC/Si HyS have been presented^[48, 57, 59, 62], as illustrated in Fig. 7. The curves of Si IGBT and SiC MOSFET intersect at one point, which is called the sweet point. Below the sweet point, most of the current flows through SiC MOSFET. Above the sweet point, the Si IGBT shares more current. Therefore, at either a high or low current, the

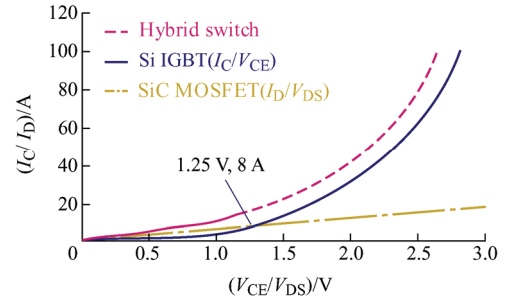


Fig. 7 Output characteristics (I_C , I_D versus V_{CE} , V_{DS}) of Si IGBT, SiC MOSFET, and HyS

HyS has a lower conduction loss. A detailed model for evaluating the conduction loss of Si IGBT + SiC MOSFET HyS has also been established^[65].

For switching loss, to fully utilize the fast switching speed of SiC MOSFET, a switching scheme was proposed^[57], as depicted in Fig. 8. Si IGBT and SiC MOSFET are turned on at the same time, although Si IGBT is turned off earlier. After a delay time T_d , the SiC MOSFET is turned off. Consequently, a zero-voltage switching (ZVS) of Si IGBT is achieved, and the switching loss is significantly reduced. It is worth mentioning that the delay time T_d needs to be designed in accordance with the turn-off loss of Si IGBT, and the conduction loss of SiC MOSFET. The switching frequency and efficiency of the converter will also be influenced by delay time T_d . Some factors worthy of consideration for setting the delay time have been described^[66].

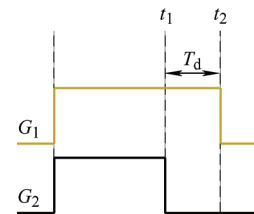


Fig. 8 Gate driver signal of HyS in Ref. [58]

The third aspect is the switching pattern of HyS. Recent studies^[48, 59, 67-68] have presented and compared several gate control options. A comprehensive switching pattern scheme, based on the load current to reduce losses, enhance the overload capability, and guarantee the operational reliability was developed^[57]. A new gate control optimization to keep the junction temperature within the specified temperature range has been proposed^[69].

The fourth aspect is the current sharing behavior in Si IGBT + SiC MOSFET HyS. The influence of the

different delay times on the current sharing has been presented^[70-71].

The mechanisms of the current sharing between Si IGBT and SiC MOSFET during the turn-off period have been discussed^[72]. Both mathematical model and theoretical calculation of the current sharing for the HyS were presented^[73]. The effect of the conductivity modulation on the current sharing for the HyS was also analyzed^[73].

The fifth aspect is the inductance of the parasitic interconnect in the HyS. The parallel interconnection of Si IGBT and SiC MOSFET introduces a parasitic inductance on each device. The distribution of parasitic inductance can be symmetrical or asymmetrical, but will cause a dynamic unbalanced current. A parasitic interconnect inductance model has also been presented^[59, 67]. According to the value of parasitic interconnect inductance, an optimal gate control can be used.

3.1.3 Si IGBT/MOSFET + GaN HEMT

Similar with SiC MOSFET, GaN HEMT has an ultra-fast switching speed and outstanding junction temperature capabilities^[59]. The high cost and low current grade of the product limit the full replacement of the Si IGBT with GaN HEMT. Therefore, the HyS consists of a GaN HEMT and a Si device is a cost-effective solution instead of using a full GaN HEMT. There are two main types of GaN HEMT + Si HyS, one is a GaN HEMT + Si IGBT HyS and the other one is a GaN HEMT + Si MOSFET HyS.

For a GaN HEMT + Si IGBT HyS, the analysis is the same as for a SiC MOSFET + Si IGBT HyS, as discussed in the previous section^[1, 48]. A GaN HEMT+ Si MOSFET HyS formed by two SMT GaN HEMTs and a Si MOSFET in parallel, as shown in Fig. 9, was previously proposed^[34]. The low on-state resistance of a Si MOSFET needs to be selected because it will undertake most of the current during the on-state and dead-time periods.

Although gate control strategies vary, all such schemes must follow a certain rule, i.e., the Si MOSFET should be turned off earlier than the GaN HEMT to achieve a ZVS turn-off of the Si MOSFET and make full use of the excellent switching characteristics of the GaN HEMT to optimize the

overall switching loss of the system. The equivalent circuit and theoretical analysis of the switching process have been presented^[34]. A comparison of the switching losses between SiC MOSFET-HyS and GaN HEMT-HyS has been discussed in Refs. [74-75]. Under identical experimental conditions, the total switching losses of the GaN-based hybrid switch are lower than that of the SiC-based hybrid switch. Beyond that, the switching frequency of a GaN-based HyS can reach three times of a Si IGBT.

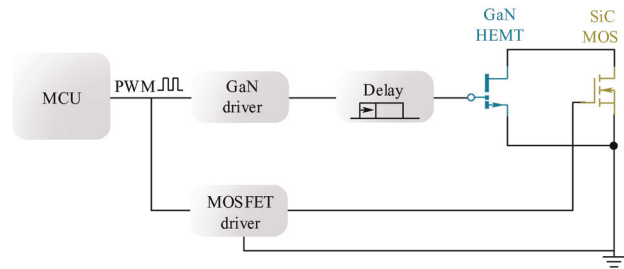


Fig. 9 GaN HEMT+ Si MOSFET HyS

3.2 Modular level application

For the previous hybrid applications, they are all based on discrete devices. Furthermore, to meet the higher efficiency and higher power density requirements, hybrid modules were proposed. Compared with discrete devices, hybrid modules can operate at a higher temperature, reduce the parasitic inductance, and enhance the power level.

The combination of a Si IGBT and a SiC SBD, such as an Infineon hybrid module FF600R12IS4F and Fuji electric hybrid module 6MSI100VB-120-50, is the most commercially available type of hybrid module. Such a hybrid switch module has been proposed in many studies, and the high performance of a hybrid switch module was validated^[74-77].

A SiC-based hybrid module and a full-Si module were compared in terms of the turn-on behavior, reverse recovery behavior, turn-off loss, and radiation noise^[78]. Here, the turn-on and reverse recovery losses definitely much lower than those of a full-Si module. For the hybrid module, the spike voltage caused by the turn-off process is smaller owing to the reduced forward recovery voltage drop. In addition, hybrid modules are more suitable for operating at a higher frequency. Furthermore, the hybrid module is a strong competitor at high temperatures^[79-80]. The standard

half-bridge hybrid module composed of Si IGBTs and SiC SBDs is depicted in Fig. 10.

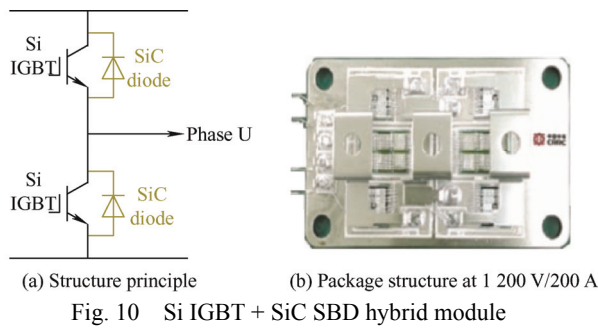


Fig. 10 Si IGBT + SiC SBD hybrid module

A simple design and development of a Si IGBT + SiC SBD hybrid module was previously described^[80], including the selection of SiC SBD diodes, the layout of direct bonded copper (DBC), and the direct cooling plate. In contrast to a conventional combination, a novel half-bridge 3.3 kV/450 A hybrid module with two anti-parallel SiC SBDs for each Si IGBT was proposed^[81]. Further, using Si IGBT with fast switching characteristics in a hybrid module to improve the performance and enhance the reliability has been reported^[54].

Many scholars have studied the hybrid module of Si IGBT and SiC MOSFET. However, there is no commercial product. The detailed design procedures of a 1 200 V/200 A SiC/Si hybrid module were presented^[82-83], where each leg includes two identical Si IGBTs, one SiC MOSFET, and one Si Diode. A comparison of the power losses and costs is addressed between Si IGBT, SiC MOSFET, and hybrid modules. It was concluded that a hybrid module can achieve the best cost as well as the lowest loss. To further increase the current level, a 1 200 V/400 A SiC/Si hybrid module was developed^[84-85], and each phase leg consists of two 1 200 V/200 A Si IGBTs, two 1 200 V/50 A SiC MOSFETs, and two 1 200 V/100 A Si diodes.

A 6.5 kV hybrid module concept is developed based on Si IGBT and SiC JFET as an ideal next step for high-voltage applications^[61]. Compared with Si IGBT-based converters, the switching losses can be reduced by over 70%, but the cost is increased by approximately 70%. Similarly, a 6.5 kV SiC/Si hybrid module, called a FREEDM-Pair, was proposed and has been regarded as an excellent candidate for high-power applications^[51]. Different configurations, such as SiC MOSFET-based hybrid module and a SiC

JFET-based hybrid module, were compared. The aforementioned hybrid module is employed in an H-bridge topology. For other complicated topologies, such as a T-type 3L topology, hybrid modules require a special customization that increases the cost but still achieves a high efficiency at a high power level^[66].

For use in a fast charging electric vehicle, GaN HEMT + Si MOSFET hybrid module was applied in dual active bridge (DAB) DC/DC converters^[86]. The hybrid module has larger heat-dissipating areas in contrast to a full GaN module, which means an enhanced thermal capacity performance can be achieved.

4 Overview of circuit-level application

In addition to the abovementioned hybrid applications, a circuit-level hybrid application is also an important branch. In the following subsections, the essence of the hybrid structure is described, and several respective circuits are investigated and compared.

4.1 Essence of hybrid converter

In recent years, several types of SiC/Si hybrid multilevel converters are proposed^[86-87], mainly including 3L-ANPC and five-level (5L) ANPC converter. To develop more hybrid multilevel converters for medium-voltage high-speed drive systems, the SiC/Si hybrid converter topology generation mechanism must be fully investigated. The essence of SiC/Si hybrid structure, taking the 3L-ANPC as an example, was investigated in two articles.

First, a switch cell (SC) was utilized to explain the reason why the ANPC converter can be decoupled into two parts^[66], including a high-frequency part and a low-frequency part. A similar idea can be found elsewhere^[88].

As is well-known, a multilevel converter can utilize series-connected capacitors on the DC side, which is called the voltage clamping cell, to generate multiple voltage levels, as given in Fig. 11. In addition, the operation of a multilevel converter can also be described as a single-pole multiple throw switch, i.e., an SC.

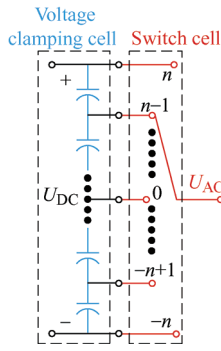


Fig. 11 Scheme of multilevel converter

For SiC/Si hybrid multilevel converters, the SC can be divided into a selection SC (SSC) and commutation SC (CSC), as shown in Fig. 12. The SSC acts like a multiplexer that creates the connection between the voltage levels $\{n, n-1, \dots, -n+1, -n\}$ and the two terminals a and b . By contrast, the CSC works like a single pole double throw switch that realizes a high-frequency voltage level commutation between a and b . Therefore, Si IGBTs can be applied to the SSC and SiC MOSFETs can be applied to the CSC.

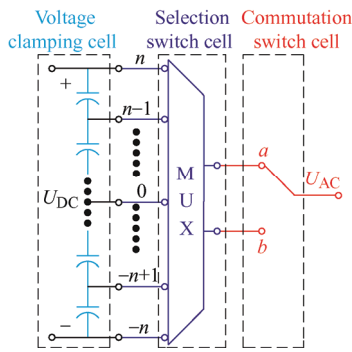


Fig. 12 Scheme of the hybrid converter

From a previous analysis, it is natural to derive the SiC/Si hybrid 3L-ANPC converter with two SiC MOSFETs and four Si IGBTs, which is also called a 2-SiC hybrid 3L-ANPC^[89], as shown in Fig. 13. However, a major concern for this derivation is that the SiC/Si hybrid 3L-ANPC converter with four SiC MOSFETs and two Si IGBTs, called a 4-SiC hybrid 3L-ANPC^[89], cannot be generated, as shown in Fig. 14.

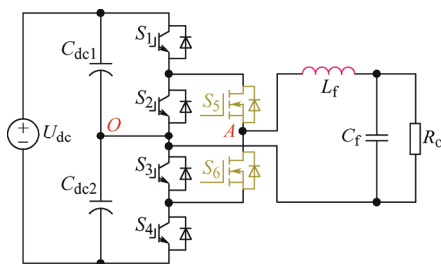


Fig. 13 2-SiC hybrid 3L-ANPC topology

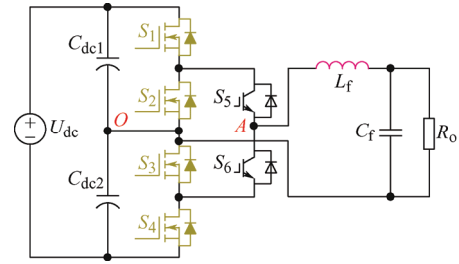
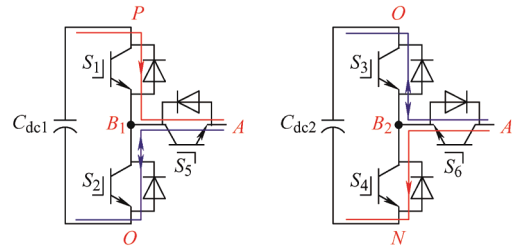


Fig. 14 4-SiC hybrid 3L-ANPC topology

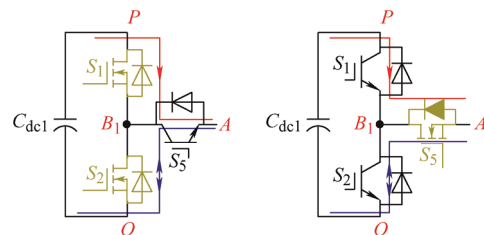
The idea of generating a new SiC/Si hybrid topology was proposed^[89]. The 3L-ANPC inverter can be split into positive and negative switching cells, called P-ANPC and N-ANPC^[89], respectively, as shown in Fig. 15. Taking the P-ANPC as an example for analysis, according to the direction of the inductive current, it can be divided into the freewheeling mode and the active mode. The current path should be guaranteed to be composed of a SiC MOSFET and a Si IGBT in series, regardless of whether in active or freewheeling mode. As a result, two types of P-ANPC SiC/Si hybrid switching cells are developed, as depicted in Fig. 16a and Fig. 16b^[89].



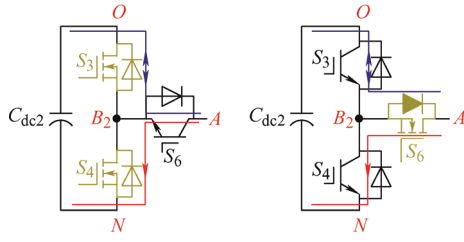
(a) P-ANPC switching cell (b) N-ANPC switching cell

Fig. 15 ANPC switching cells

Furthermore, there are also two types of N-ANPC, as shown in Fig. 16c and Fig. 16d. The 2-SiC hybrid 3L-ANPC converter topology can be generated by a type-II SiC/Si hybrid P-ANPC switching cell and a type-II SiC/Si hybrid N-ANPC switching cell, as illustrated in Fig. 13. In addition, the 4-SiC hybrid 3L-ANPC converter topology can be generated using a type-I SiC/Si hybrid P-ANPC switching cell and a type-I SiC/Si hybrid N-ANPC switching cell, as depicted in Fig. 14. The systematic method will guide



(a) Type-I of P-ANPC (b) Type-II of P-ANPC



(c) Type-I of N-ANPC (d) Type-II of N-ANPC

Fig. 16 Four types of the SiC/Si hybrid ANPC switching cells the derivation of more hybrid multilevel converters with more voltage levels.

4.2 Overview of WBG/Si hybrid applications

4.2.1 Hybrid applications under 3L-ANPC

Several WBG/Si hybrid converters are summarized in this section, and the corresponding modulation schemes are introduced from a different perspective.

For 3L-ANPC converters, many hybrid topologies and modulation schemes have been proposed^[33, 36, 66, 89-92]. Based on the previous analysis, two typical SiC/Si hybrid topologies can be depicted as in Fig. 13 and Fig. 14. For the 2-SiC hybrid 3L-ANPC converter, an extremely high-efficient modulation scheme was proposed^[86].

Fig. 17 shows the waveforms of a 2-SiC hybrid 3L-ANPC inverter modulation scheme^[36]. At the positive half voltage cycle, S_1 and S_3 are on, S_2 and S_4 are off, and SiC MOSFETs S_5 and S_6 are complementary pairs with a switching frequency. In addition, according to the symmetry of the circuit, at the negative half voltage cycle, S_1 and S_3 are off, S_2 and S_4 are on, and SiC MOSFETs S_5 and S_6 have high-frequency switching complementarity.

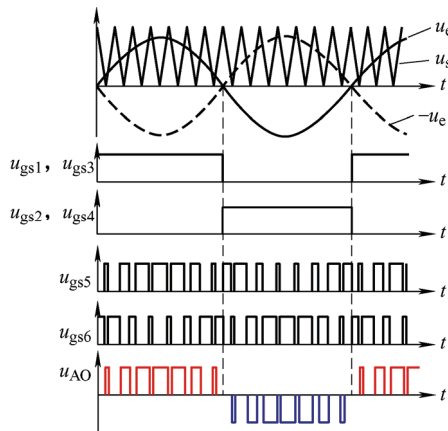


Fig. 17 Waveforms of 2-SiC hybrid 3L-ANPC modulation scheme

Another 2-SiC hybrid scheme was proposed, as illustrated in Fig. 18^[90]. Correspondingly, two

modulation strategies are used to concentrate the switching losses on two SiC MOSFETs, as given in Figs. 19^[90] and 20^[90]. Although there are Si IGBTs with high-frequency switching in both modulations, they are operating under ZVS or zero-current switching (ZCS). After an experimental verification^[90], the former 2-SiC hybrid scheme is slightly more efficient than the latter. As the common idea of these 2-SiC hybrid schemes, almost all switching losses are moved to two SiC MOSFETs such that the switching losses are greatly reduced, and a high efficiency is achieved.

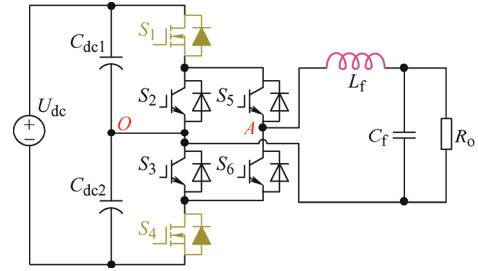


Fig. 18 2-SiC hybrid 3L-ANPC topology

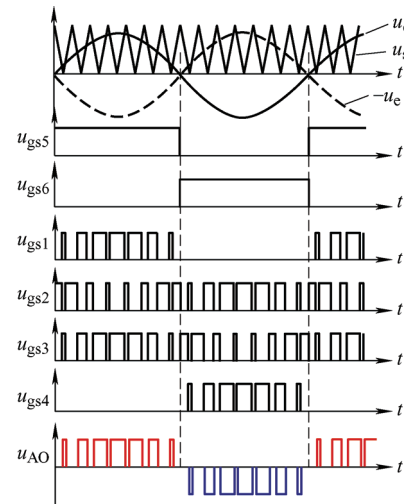


Fig. 19 Waveforms of 2-SiC modulation scheme I

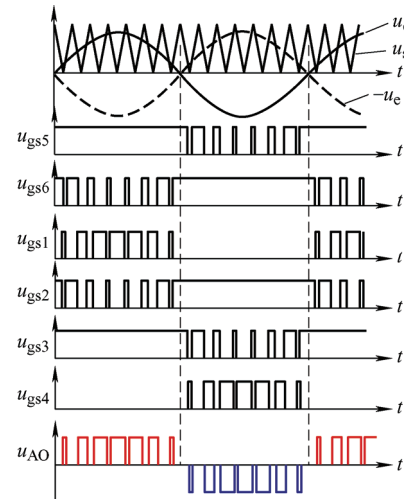


Fig. 20 Waveforms of 2-SiC modulation scheme II

A megawatt-scale medium-voltage inverter based on a 3L-ANPC with a hybrid utilization of four SiC MOSFETs and two Si IGBTs, as shown in Fig. 14, has also been developed^[35]. Specifically, at the positive half voltage cycle, S_5 is in an ON state, and the gating signals of S_1 and S_3 are the same. SiC MOSFETs S_1 and S_2 are complementary pairs with the switching frequency. At the negative half voltage cycle, the gating signals of S_2 and S_4 are the same, S_6 is on, and S_3 and S_4 are complementary pairs with the switching frequency, as illustrated in Fig. 21^[35, 91]. A similar modulation can be found elsewhere^[91]. With this modulation, all commutations will take place between two SiC devices in the same module to minimize the commutation loop inductance. In addition, the loss distribution is more balanced compared to the 2-SiC hybrid scheme.

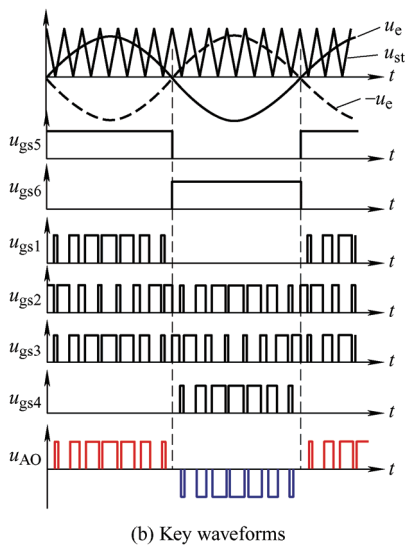
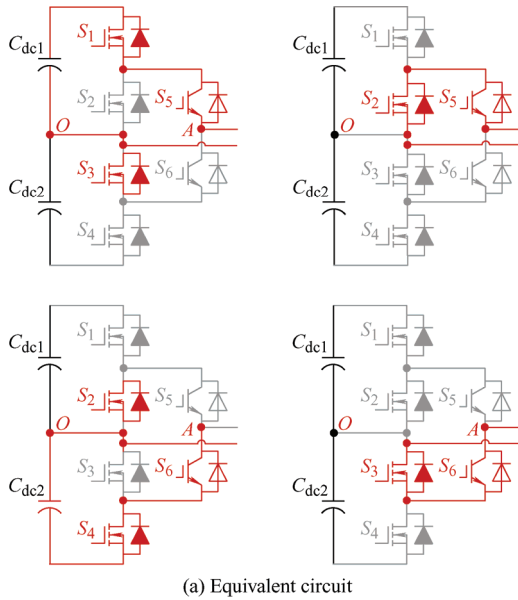


Fig. 21 Basic states of 4-SiC modulation scheme I

In addition, another modulation scheme for a

4-SiC hybrid 3L-ANPC converter, which is called the 4-SiC modulation scheme II, was illustrated^[92]. The specific equivalent circuit and a gating signal are shown in Figs. 22a and 22b, respectively. Compared with the modulation scheme I, S_3 is always in an ON state during a positive half cycle, and S_2 is ON in a negative half cycle. In rectifier mode, the charging and discharging losses of junction capacitors with modulation scheme II is slightly less than that of the modulation scheme I. In inverter mode, however, a large reverse recovery current and reverse recovery losses will be generated in the anti-parallel diodes of two Si IGBTs. Consequently, the total losses of modulation scheme-II are slightly higher compared to those of the modulation scheme-I.

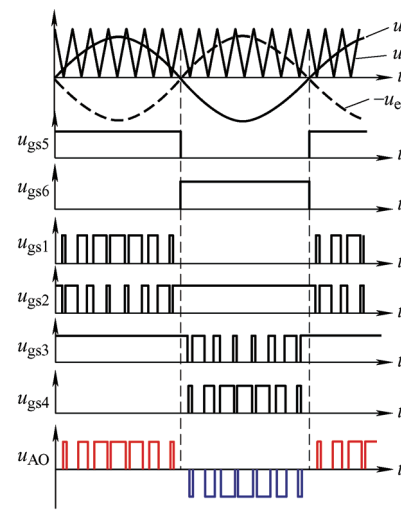
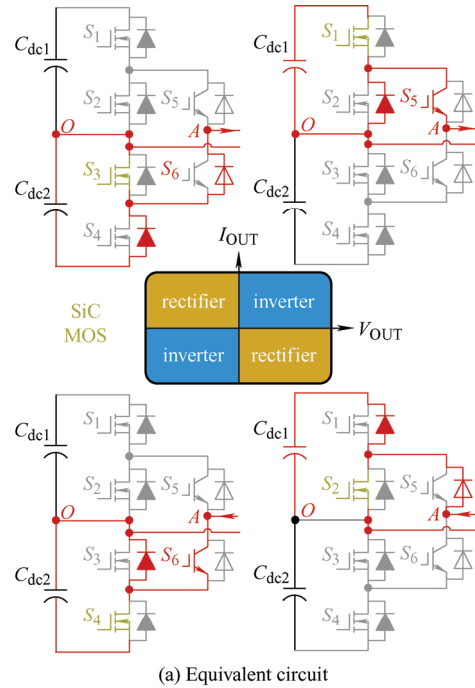


Fig. 22 Basic states of 4-SiC modulation scheme II

A third modulation scheme, called the 4-SiC modulation scheme III, was developed^[93-95]. Unlike modulation scheme I and modulation scheme II, this modulation involves a large commutation loop. Fig. 23^[93] shows the equivalent circuit at the positive half cycle. To achieve a better thermal and loss balance, this method can be employed. However, from an efficiency standpoint, two Si IGBTs are hard switches which exist high switching losses and high voltage spikes issues, particularly in high power applications.

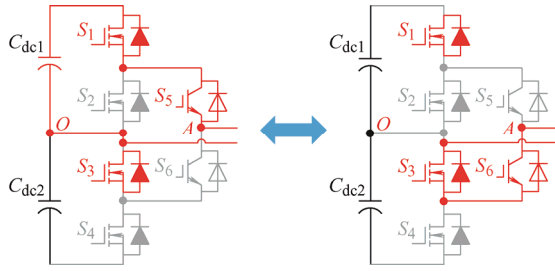


Fig. 23 Commutation process of the 4-SiC modulation scheme III

Recently, the efficiency, power density, and thermal balance of the aforementioned application scheme are analyzed and compared in detail^[89]. From the perspective of efficiency, the 2-SiC is the highest, the 4-SiC with modulation scheme-I is the second-highest, and the 4-SiC with modulation scheme-II is the lowest. Under the same circumstances, the 4-SiC hybrid 3L-ANPC inverter with modulation scheme-I can realize a higher power density and better thermal balance. Thus, the 4-SiC hybrid 3L-ANPC inverter using modulation scheme-I is applicable to high-power and high-power density applications, and the 2-SiC hybrid 3L-ANPC inverter is suitable for cost-effective applications.

Furthermore, a three-phase system is necessary to increase the power level. A three-phase 2-SiC hybrid 3L-ANPC converter^[66] is shown in Fig. 24, a dedicated space vector modulation (SVM) scheme for which was previously proposed^[66]. Only one-third of the switching devices in the converter are SiC MOSFETs. Therefore, the total cost is much lower than that of all SiC-based converters whereas the efficiency still performs well.

A three-phase 4-SiC hybrid 3L-ANPC inverter for aircraft hybrid-electric propulsion applications was developed^[96]. The commutation process is the same as that shown in Fig. 20. However, when the load is a

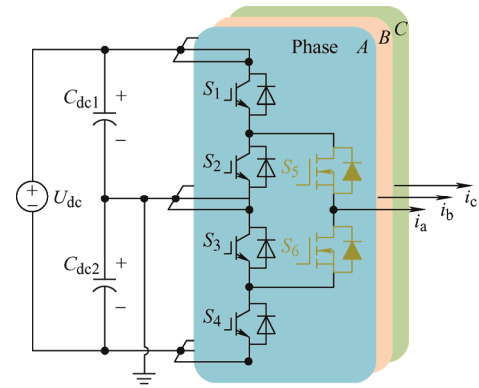


Fig. 24 Three-phase circuit of 2-SiC hybrid ANPC converter

motor, a pump-back test is necessary to validate the capability, thermal design, and basic control functions. Based on this condition, the test of the SiC/Si hybrid converter was discussed and a test report was given^[96]. Moreover, a three-phase megawatt SiC/Si hybrid converter, as shown in Fig. 25, with a 2.4 kV bus voltage and 99% efficiency was proposed^[97]. Its single-phase structure is still composed of four SiC MOSFETs and two Si IGBTs. The modulation of the converter adopts the same scheme as described elsewhere^[35], but differing from this approach, in the present study, higher power switching devices were employed to realize a high-efficiency power transformation at a megawatt-level and provide the matching hardware design. It can provide guidance to SiC/Si hybrid schemes for multi-electric aircraft applications.

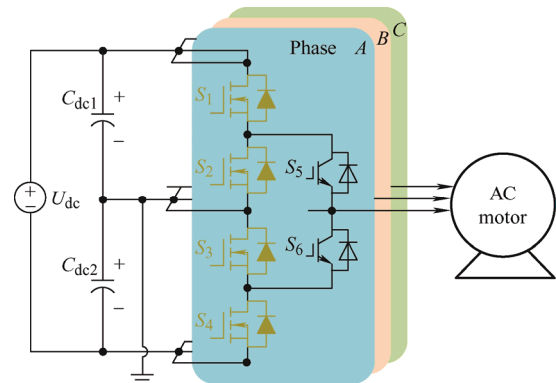


Fig. 25 Three-phase circuit of 4-SiC hybrid ANPC converter

4.2.2 Hybrid applications under 5L-ANPC

Clearly, in multilevel converters, such as 5L, the hybrid utilization of WBG/Si devices can significantly reduce the filter volume and increase the power density. A 5L full-bridge (FB) topology is clearly shown in Fig. 26^[98].

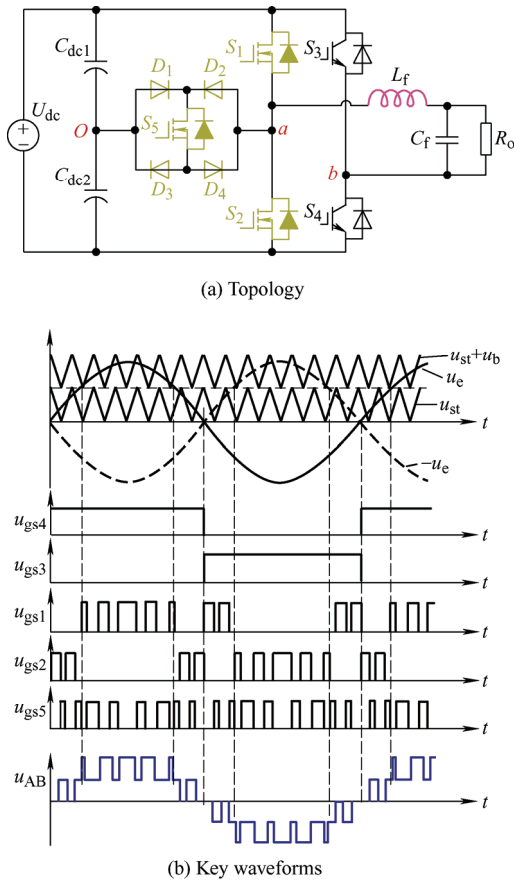


Fig. 26 Hybrid 5L-ANPC full-bridge inverter and its two modulation schemes

The clamp bidirectional switching components are all composed of SiC devices, and the switching devices on the grid-frequency bridge arm are composed of Si IGBT. Two modulation schemes are also presented in this paper, and it is concluded through an analysis that both modulation schemes achieve a better performance than the all Si-based one, whereas modulation scheme II has a lower THD. However, the above topology employs three SiC MOSFET and four SiC SBDs. Although the cost is lower than that of the SiC-based prototype, the overall cost is still high for the 5L topology.

As a result, a 5L ANPC full-bridge topology with a 4SiC/2Si hybrid scheme was proposed, as shown in Fig. 27^[99]. By employing the novel modulation scheme, some switching actions are added to decrease the conduction loss. However, the added switching actions are all soft-switching, and thus a tradeoff between the added additional losses and the optimized conduction losses is achieved. Consequently, the overall efficiency of the converter is improved, and the cost is reduced by 45% compared with a previously

described hybrid scheme^[98].

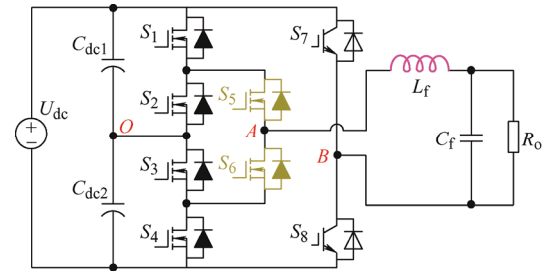


Fig. 27 2-SiC hybrid 5L-ANPC full-bridge inverter

4.2.3 Hybrid applications under special circuits

The above hybrid scheme is mostly used for inverter mode. For rectifier mode, a WBG/Si hybrid scheme also has certain advantages. A totem-pole PFC is well known as the simplest topology among all the bridgeless boost PFC structures^[100]. Owing to the reverse recovery effect of the body diodes of Si MOSFET, the efficiency and operating frequency of a traditional totem-pole PFC rectifier are limited. The emergence of GaN devices makes a totem-pole PFC topology popular^[101-104]. Because the GaN HEMT has a high turn-on loss, an extremely small turn-off loss, and a small reverse recovery loss, the GaN-based totem-pole PFC under continuous conduction mode (CCM) can still reach 99% peak efficiency at a 1 kW power level by limiting the switching frequency to approximately 100 kHz or under^[105]. A GaN-based MHz PFC rectifier under critical conduction mode (CRM) was proposed to achieve a ZVS turn-on based on an off-time extension, as shown in Fig. 28^[105]. Two-phase interleaving control for an input current ripple cancellation and an EMI filter size reduction was applied. With a ZVS extension, the entire line cycle of the ZVS is achieved to improve the efficiency.

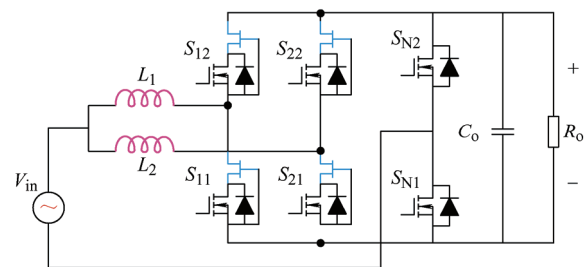


Fig. 28 Two-phase interleaved totem-pole PFC with cascade GaN devices

A 3L rectifier consisting of a SiC MOSFET and

Si diode was proposed^[106]. Through a specific modulation scheme, the reverse recovery issues of all Si diodes are eliminated. The topology and its modulation scheme are illustrated in Fig. 29^[106]. Consequently, it has a higher efficiency than the rectifier composed of SiC MOSFETs and Si IGBTs. Meanwhile, the total device cost of the rectifier is much lower than that of all SiC-based rectifiers.

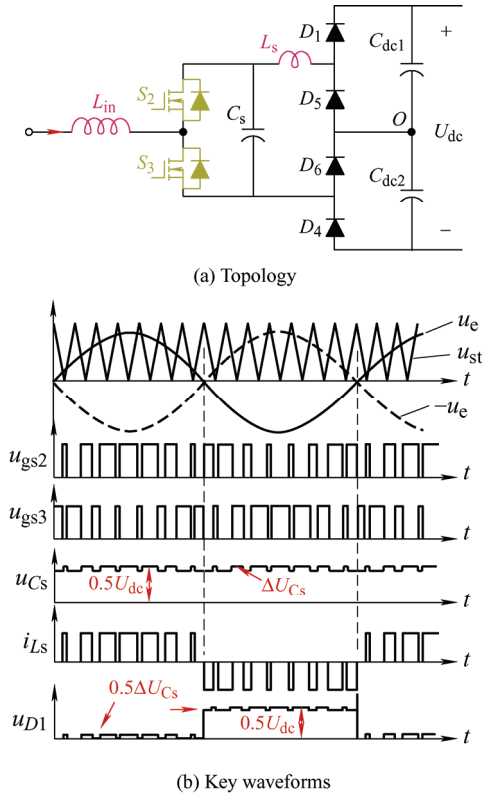


Fig. 29 SiC MOSFET and Si diode hybrid three-level rectifier and its modulation scheme

Not only DC/AC or AC/DC converters but also AC/AC converters or three-port converters can employ a WBG/Si hybrid scheme. As shown in Fig. 30, a 3L three-leg converter based on the T-type structure was proposed^[107]. Unlike the previous bridge structure, the switching devices bearing a high-voltage stress are replaced by SiC MOSFETs, whereas other switching devices are still Si devices. The high-frequency switching actions are moved to the SiC devices. Thus, the overall loss is reduced. The results show that this hybrid scheme improves the efficiency by 0.5% compared with the Si-based prototype.

Based on the aforementioned discussion, it can be found that most of the high-frequency switching

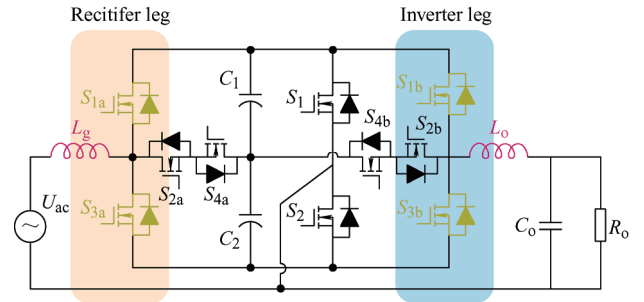


Fig. 30 SiC/Si hybrid AC/AC converter

actions should be moved to the WBG devices when using the WBG/Si hybrid scheme regardless of what the circuit topologies are. When it is necessary to adopt the WBG/Si hybrid scheme, it is suggested to propose a corresponding modulation scheme to maximize the advantages of WBG devices.

4.3 Summary and comparison

According to the aforementioned analysis, a hybrid WBG/Si device utilizes a tradeoff between performance and cost of the power converters. For the circuit level utilization scheme, if the efficiency is improved while the cost is not significantly increased, the hybrid scheme is seen as successful. To demonstrate the effectiveness of existing schemes, a variable called the efficiency-consumption ratio is defined in this section, the expression of which is as follows

$$\Delta ECr = \frac{P_{\text{rate}} \times (\eta_{\text{hybrid}} - \eta_{\text{pure_si}})}{C_{\text{hybrid}} - C_{\text{pure_si}}} \quad (1)$$

where η_{hybrid} and $\eta_{\text{pure_si}}$ represent the rated efficiency with hybrid devices and the efficiency with pure Si devices, respectively. Here, C_{hybrid} and $C_{\text{pure_si}}$ represent the cost with hybrid devices and the cost with pure Si devices, respectively. In addition, P_{rate} represents the rated power of the converter.

the efficiency and cost of various schemes according to a previous study and data are summarized in Tab. 1. The efficiency of the hybrid and pure Si schemes under the same working conditions were compared, and a cost comparison was also included. Clearly, full-SiC converters are the most expensive, and full-Si converters are the least expensive. In addition, WBG/Si hybrid converters can achieve a good tradeoff between efficiency and cost.

Tab. 1 Comparison of hybrid WBG/Si scheme

Scheme	(Hybrid/Si) Efficiency (%)	Pure Si total cost /RMB	Hybrid total cost /RMB	Pure SiC total cost /RMB	Scheme	(Hybrid/Si) Efficiency (%)	Pure Si total cost /RMB	Hybrid total cost /RMB	Pure SiC total cost /RMB
[66]-2L	(98.2/94.6) (@50 kHz, 50 kW)	220	870	1 519	[90]-A	(98.9/97.9) (@16 kHz, 3.3 kW)	168	359	742
[66]-3L	(98.8/97.4) (@50 kHz, 50 kW)	440	1 739	3 038	[90]-B	(98.9/97.9) (@16 kHz, 3.3 kW)	168	359	742
[86]	N/A	546	800	1 053	[35], [91], [97]	(99.1/98) (@20 kHz, 1 MW)	6 397	13 105	16 459
[89] 4SiC	(97.8/97.4) (@40 kHz, 2 kW)	125	260	327	[106]	(99/98) (@30 kHz, 4.2 kW)	192	693	840
[89] 2SiC	(97.9/97.4) (@40 kHz, 2 kW)	125	193	327	[98]	(98.97/98) (@N/A, 500 W)	153	291	349
[36] MOS	(99.1/98) (@30 kHz, 4 kW)	91	250	389	[99]	(96.5/95.2) (@40 kHz, 4 kW)	156	233	436
[36] IGBT	(98.8/97.9) (@30 kHz, 4 kW)	51	164	389	[107]	(98.9/98.7) (@30 kHz, 3 kW)	266	339	412

The efficiency-consumption ratio curve of each scheme is shown in Fig. 31. It can be seen that the hybrid scheme^[35] achieves the greatest benefit, whereas even a scheme with a lower efficiency-consumption ratio^[98] of higher than zero achieves a good tradeoff between performance and cost. Therefore, the hybrid application of WBG/Si devices is an alternative to improving the performance of the converter when the price of WBG devices remains high.

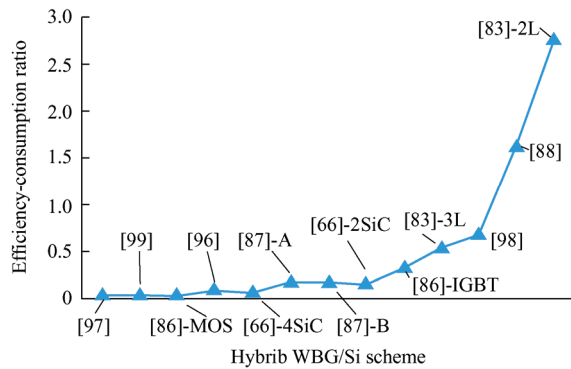


Fig. 31 Efficiency-consumption ratio curve of existing solutions

5 Conclusions

In recent years, WBG devices, as represented by a SiC and a GaN, have attracted increased attention owing to their outstanding performance and have become a research hotspot of many research institutions and companies. However, owing to the high price of wide bandgap devices, it is impossible to replace all switching devices with

WBG devices in current industrial applications. If a partial-WBG converter can achieve the same effect as a full-WBG converter, the cost can be greatly reduced, and the efficiency can be higher than in a full-Si converter. In this paper, the differences between WBG and Si devices were compared, and the hybrid scheme at the device, modular, and circuit levels were comprehensively viewed. However, at the same time, there are still many challenges to overcome. First, a more serious EMI problem will be introduced owing to the fast switching speed of WBG devices. Second, WBG devices with a high blocking voltage have not been commercialized, and their performance has yet to be optimized. Third, compared with Si devices, wide gap devices have a lower reliability, greater short-circuit current, and shorter short-circuit current tolerance time. Fourth, WBG devices presently have high market prices. Fifth, the high dv/dt and di/dt of WBG devices will occur if stray inductance and capacitor are not minimized in a power circuit design.

Future research challenges based on WBG/Si hybrid utilization are as follows.

- (1) Application scheme of WBG/Si in DC/DC converter.
- (2) Higher frequency WBG/Si modulation scheme.
- (3) WBG/Si hybrid scheme in multilevel AC/DC converter.
- (4) Better loss and thermal balance performance to achieve high power.

References

- [1] C Wang, L Yang, Z Wang, et al. Circuit configuration and control of a grid-tie small-scale wind generation system for expanded wind speed range. *IEEE Transactions on Power Electronics*, 2017, 32(7): 5227-5247.
- [2] L Zhang, K Sun, Y Xing, et al. A family of five-level dual-buck full-bridge inverters for grid-tied applications. *IEEE Transactions on Power Electronics*, 2016, 31(10): 7029-7042.
- [3] M Abarzadeh, K Al-Haddad. An improved active-neutral-point-clamped converter with new modulation method for ground power unit application. *IEEE Transactions on Industrial Electronics*, 2019, 66(1): 203-214.
- [4] X Zhou, B Zhou, K Wang, et al. Two-step rotor position estimation method for doubly salient electromagnetic starter-generator over zero and low speeds range. *IEEE Journal of Emerging and Selected Topics in Power Electronics*, DOI: 10.1109/JESTPE.2020.2991112.
- [5] M Yilmaz, P T Krein. Review of battery charger topologies, charging power levels, and infrastructure for plug-in electric and hybrid vehicles. *IEEE Transactions on Power Electronics*, 2013, 28(5): 2151-2169.
- [6] M Schweizer, J W Kolar. Design and implementation of a highly efficient three-level T-type converter for low-voltage applications. *IEEE Transactions on Power Electronics*, 2013, 28(2): 899-907.
- [7] M S Ortmann, S A Mussa, M L Heldwein. Three-phase multilevel PFC rectifier based on multistate switching cells. *IEEE Transactions on Power Electronics*, 2015, 30(4): 1843-1854.
- [8] J Li, J Liu, D Boroyevich, et al. Three-level active neutral-point-clamped zero-current-transition converter for sustainable energy systems. *IEEE Transactions on Power Electronics*, 2011, 26(12): 3680-3693.
- [9] Y Guan, Y Wang, Q Bian, et al. High-efficiency self-driven circuit with parallel branch for high frequency converters. *IEEE Transactions on Power Electronics*, 2018, 33(2): 926-931.
- [10] S Park, Y Sohn, G Cho. SiC-based 4 MHz 10 kW ZVS inverter with fast resonance frequency tracking control for high-density plasma generators. *IEEE Transactions on Power Electronics*, 2020, 35(3): 3266-3275.
- [11] A Jafari, M S Nikoo, F Karakaya, et al. Enhanced DAB for efficiency preservation using adjustable-tap high-frequency transformer. *IEEE Transactions on Power Electronics*, 2020, 35(7): 6673-6677.
- [12] A Pal, K Basu. A soft-switched high-frequency link single-stage three-phase inverter for grid integration of utility scale renewables. *IEEE Transactions on Power Electronics*, 2019, 34(9): 8513-8527.
- [13] H F Ahmed, H Cha. A new class of single-phase high-frequency isolated Z-Source AC-AC converters with reduced passive components. *IEEE Transactions on Power Electronics*, 2018, 33(2): 1410-1419.
- [14] M Mohammadi, E Adib, M R Yazdani. Family of soft-switching single-switch PWM converters with lossless passive snubber. *IEEE Transactions on Industrial Electronics*, 2015, 62(6): 3473-3481.
- [15] H Xiao, L Zhang, Z Wang, et al. A new soft-switching configuration and its application in transformerless photovoltaic grid-connected inverters. *IEEE Transactions on Industrial Electronics*, 2018, 65(12): 9518-9527.
- [16] J Fang, M Shi, H Xiao, et al. A zero-voltage-transition H5-Type transformerless photovoltaic grid-connected inverter. *IEEE Access*, DOI: 10.1109/ACCESS.2019.2946976.
- [17] D Zheng, Y Kang, H Cao, et al. Monitoring of SiC MOSFET junction temperature with on-state voltage at high currents. *Chinese Journal of Electrical Engineering*, 2020, 6(3): 1-7.
- [18] J Prakash, M Veerachary. Zero-voltage zero-current transition network for dual phase interleaved converter. *IEEE Transactions on Industry Applications*, 2020, 56(4): 3940-3953.
- [19] Z Zeng, W Shao, B Hu, et al. Chances and challenges of photovoltaic inverters with silicon carbide devices. *Proceedings of the CSEE*, 2017, 37(1): 221-233.
- [20] X Zhang, G Sheh. Implementation of 1.7 kV silicon carbide metal oxide semiconductor field effect transistors in auxiliary power supplies for industrial applications. *Chinese Journal of Electrical Engineering*, 2020, 6(3): 46-55.
- [21] C N Ho, H Breuninger, S Pettersson, et al. A comparative performance study of an interleaved boost converter using commercial Si and SiC diodes for PV applications. *IEEE Transactions on Power Electronics*, 2013, 28(1): 289-299.
- [22] Y Shi, L Wang, R Xie, et al. A 60-kw 3-kW/kg five-level T-type SiC PV inverter with 99.2% peak efficiency. *IEEE Transactions on Industrial Electronics*, 2017, 64(11): 9144-9154.
- [23] Y Shi, R Xie, L Wang, et al. Switching characterization and short-circuit protection of 1200 V SiC MOSFET T-type module in PV inverter application. *IEEE Transactions on Industrial Electronics*, 2017, 64(11): 9135-9143.
- [24] L Wang, Y Shi, Y Shi, et al. Ground leakage current

- analysis and suppression in a 60-kW 5-level T-type transformerless SiC PV inverter. *IEEE Transactions on Power Electronics*, 2018, 33(2): 1271-1283.
- [25] Z Liu, B Li, F C Lee, et al. High-efficiency high-density critical mode rectifier/inverter for WBG-device-based on-board charger. *IEEE Transactions on Industrial Electronics*, 2017, 64(11): 9114-9123.
- [26] E Gurpinar, A Castellazzi. Single-phase T-type inverter performance benchmark using Si IGBTs, SiC MOSFETs, and GaN HEMTs. *IEEE Transactions on Power Electronics*, 2016, 31(10): 7148-7160.
- [27] F Wang, Z Zhang. Overview of silicon carbide technology: Device, converter, system, and application. *CPSS Transactions on Power Electronics and Applications*, 2016, 1(1): 13-32.
- [28] S S Manohar, A Sahoo, A Subramaniam, et al. Condition monitoring for device reliability in power electronic converters: A review. *IEEE Transactions on Power Electronics*, 2010, 25(11): 2734-2752.
- [29] A Anthon, Z Zhang, M A E Andersen, et al. The benefits of SiC MOSFETs in a T-type inverter for grid-tie applications. *IEEE Transactions on Power Electronics*, 2017, 32(4): 2808-2821.
- [30] J Biela, M Schweizer, S Waffler, et al. SiC versus Si: Evaluation of potentials for performance improvement of inverter and DC-DC converter systems by SiC power semiconductors. *IEEE Transactions on Industrial Electronics*, 2011, 58(7): 2872-2882.
- [31] C M H Breuninger, S Pettersson, G Escobar, et al. Practical design and implementation procedure of an interleaved boost converter using SiC diodes for PV applications. *IEEE Transactions on Power Electronics*, 2012, 27(6): 2835-2845.
- [32] M Imaizumi, N Miura. Characteristics of 600, 1200, and 3300 V planar SiC-MOSFETs for energy conversion applications. *IEEE Transactions on Electron Devices*, 2015, 62(2): 390-395.
- [33] U R Vemulapati, A Mihaila, R A Minamisawa, et al. Simulation and experimental results of 3.3kV cross switch "Si-IGBT and SiC-MOSFET" hybrid. *2016 28th International Symposium on Power Semiconductor Devices and ICs*, Prague, 2016: 163-166.
- [34] G Liu, K H Bai, M McAmmond, et al. Critical short-timescale transient processes of a GaN+Si hybrid switching module used in zero-voltage-switching applications. *2017 IEEE 5th Workshop on Wide Bandgap Power Devices and Applications*, Albuquerque, NM, 2017: 93-97.
- [35] D Zhang, J He, D Pan. A megawatt-scale medium-voltage high efficiency high power density "SiC+Si" hybrid three-level ANPC inverter for aircraft hybrid-electric propulsion systems. *2018 IEEE Energy Conversion Congress and Exposition*, Portland, OR, 2018: 806-813.
- [36] Q Guan, C Li, Y Zhang, et al. An extremely high efficient three-level active neutral-point-clamped converter comprising SiC and Si hybrid power stages. *IEEE Transactions on Power Electronics*, 2018, 33(10): 8341-8352.
- [37] H Takasu. Silicon carbide devices open a new era of power electronics. *Proceedings of Technical Program of 2012 VLSI Design, Automation and Test*, Hsinchu, 2012: 1-2.
- [38] S Ohn, J Yu, R Burgos, et al. Reduced common-mode voltage PWM scheme for full-SiC three-level uninterruptible power supply with small DC-link capacitors. *IEEE Trans. Power Electron*, 2020, 35(8): 8638-8651.
- [39] S Bernet. Recent developments of high power converters for industry and traction applications. *IEEE Transactions on Power Electronics*, 2000, 15(6): 1102-1117.
- [40] J Hornberger, A B Lostetter, K J Olejniczak, et al. Silicon-carbide (SiC) semiconductor power electronics for extreme high-temperature environments. *2004 IEEE Aerospace Conference Proceedings*, Big Sky, MT, 2004: 2538-2555.
- [41] H Mhiesan, J Umuhoza, K Mordi, et al. Evaluation of 1.2 kV SiC MOSFETs in multilevel cascaded H-bridge three-phase inverter for medium-voltage grid applications. *Chinese Journal of Electrical Engineering*, 2019, 5(2): 1-13.
- [42] A Elasser, T P Chow. Silicon carbide benefits and advantages for power electronics circuits and systems. *Proceedings of the IEEE*, 2002, 90(6): 969-986.
- [43] J Millán, P Godignon, X Perpiñà, et al. A survey of wide bandgap power semiconductor devices. *IEEE Transactions on Power Electronics*, 2014, 29(5): 2155-2163.
- [44] L Navarro, A Perpina, X P Godignon, et al. Thermomechanical assessment of die-attach materials for wide bandgap semiconductor devices and harsh environment applications. *IEEE Transactions on Power Electronics*, 2014, 29(5): 2261-2271.
- [45] H A Mantooth, M D Glover, P Shepherd. Wide bandgap technologies and their implications on miniaturizing power electronic systems. *IEEE Journal of Emerging and Selected Topics in Power Electronics*, 2014, 2(3): 374-385.
- [46] J G Kassakian, T M Jahns. Evolving and emerging

- applications of power electronics in systems. *IEEE Journal of Emerging and Selected Topics in Power Electronics*, 2013, 1(2): 47-58.
- [47] A Deshpande, F Luo. Design of a silicon-WBG hybrid switch. in *Proc. 2015 IEEE 3rd Workshop on Wide Bandgap Power Devices and Applications*, Blacksburg, VA, 2015: 296-299.
- [48] A Deshpande, F Luo. Comprehensive evaluation of a silicon-WBG hybrid switch. *2016 IEEE Energy Conversion Congress and Exposition*, Milwaukee, WI, 2016: 1-8.
- [49] C Yang, Y Liang. Investigation on parallel operations of IGBTs. *Proceedings of the 1996 IEEE IECON. 22nd International Conference on Industrial Electronics, Control, and Instrumentation*, Taipei, Taiwan, China, 1996: 1005-1010.
- [50] H Wen, J Liu, X Zhang, et al. Design of high power electronic building block based on parallel of IGBTs for electric vehicle. *2008 13th International Power Electronics and Motion Control Conference*, Poznan, 2008: 1518-1522.
- [51] X Song, A Huang. 6.5 kV FREEDM-pair: Ideal high power switch capitalizing on Si and SiC. *2015 17th European Conference on Power Electronics and Applications*, Geneva, 2015: 1-9.
- [52] M Schweizer, T Friedli, J W Kolar. Comparison and implementation of a 3-level NPC voltage link back-to-back converter with SiC and Si diodes. *2010 25th Annual IEEE Applied Power Electronics Conference and Exposition (APEC)*, Palm Springs, CA, 2010: 1527-1533.
- [53] S V Araújo, P Zacharias. Perspectives of high-voltage SiC-semiconductors in high power conversion systems for wind and photovoltaic sources. *Proceedings of the 2011 14th European Conference on Power Electronics and Applications*, Birmingham, 2011: 1-10.
- [54] L Amber, K Haddad. Hybrid Si IGBT-SiC Schottky diode modules for medium to high power applications. *2017 IEEE Applied Power Electronics Conference and Exposition*, Tampa, FL, 2017: 3027-3032.
- [55] C M Johnson, M Rahimo, N G Wright, et al. Characterisation of 4H-SiC schottky diodes for IGBT applications. *35th IAS Annual Meeting and World Conference on Industrial Applications of Electrical Energy*, Rome, Italy, 2000: 2941-2947.
- [56] B Ozpineci, M S Chinthavali, L M Tolbert. A 55 kW three-phase automotive traction inverter with SiC Schottky diodes. *2005 IEEE Vehicle Power and Propulsion Conference*, Chicago, IL, 2005: 6-10.
- [57] J He, R Katebi, N Weise. A current-dependent switching strategy for SiC/Si hybrid switch-based power converters. *IEEE Transactions on Industrial Electronics*, 2017, 64(10): 8344-8352.
- [58] T Zhao, J He. An optimal switching pattern for “SiC+Si” hybrid device based voltage source converters. *2015 IEEE Applied Power Electronics Conference and Exposition*, Charlotte, NC, 2015: 1276-1281.
- [59] A Deshpande, F Luo. Practical design considerations for a Si IGBT+SiC MOSFET hybrid switch: Parasitic interconnect influences, cost, and current ratio optimization. *IEEE Transactions on Power Electronics*, 2019, 34(1): 724-737.
- [60] C Li, J Lei, Q Guan, et al. High power three-level rectifier comprising SiC MOSFET & Si diode hybrid power stage. *2018 IEEE Applied Power Electronics Conference and Exposition*, San Antonio, TX, 2018: 1-7.
- [61] A Q Huang, X Song, L Zhang. 6.5 kV SiC/Si hybrid power module: An ideal next step. *2015 IEEE International Workshop on Integrated Power Packaging*, Chicago, IL, 2015: 64-67.
- [62] P Ning, T Yuan, Y Kang, et al. Review of Si IGBT and SiC MOSFET based on hybrid switch. *Chinese Journal of Electrical Engineering*, 2019, 5(3): 20-29.
- [63] M Rahimo, F Canales, R A Minamisawa, et al. Characterization of a silicon IGBT and silicon carbide MOSFET cross-switch hybrid. *IEEE Transactions on Power Electronics*, 2015, 30(9): 4638-4642.
- [64] X Song, A Q Huang, M Lee, et al. High voltage SiC/Si hybrid switch: An ideal next step for SiC. *2015 IEEE 27th International Symposium on Power Semiconductor Devices & IC's*, Hong Kong, China, 2015: 289-292.
- [65] J W Kimball, P L Chapman. Evaluating conduction loss of a parallel IGBT-MOSFET combination. *Conference Record of the 2004 IEEE Industry Applications Conference*, Seattle, WA, USA, 2004: 1233-1237.
- [66] Y Wang, N Zhu, C Yan, et al. Efficiency improvement of 2- and 3-level inverters for distributed photovoltaic application using hybrid devices. *2015 IEEE 2nd International Future Energy Electronics Conference*, Taipei, China, 2015: 1-7.
- [67] Y Wang, M Chen, C Yan, et al. Efficiency improvement of grid inverters with hybrid devices. *IEEE Transactions on Power Electronics*, 2019, 34(8): 7558-7572.
- [68] Z Li, J Wang, X Jiang, et al. Optimal control strategies for SiC MOSFET and Si IGBT based hybrid switch. *2018 IEEE Applied Power Electronics Conference and Exposition*, San Antonio, TX, 2018: 1717-1721.
- [69] J Wang, Z Li, X Jiang, et al. Gate control optimization of SiC/Si hybrid switch for junction temperature balance and

- power loss reduction. *IEEE Transactions on Power Electronics*, 2019, 34(2): 1744-1754.
- [70] H A C Braga, I Barbi. A new technique for parallel connection of commutation cells: Analysis, design, and experimentation. *IEEE Transactions on Power Electronics*, 1997, 12(2): 387-395.
- [71] K F Hoffmann, J P Karst. Inductive decoupling of parallel connected commutation cells for dynamic current balancing. *2004 IEEE 35th Annual Power Electronics Specialists Conference*, Aachen, Germany, 2004: 3978-3983.
- [72] R A Minamisawa, U Vemulapati, A Mihaila, et al. Current sharing behavior in Si IGBT and SiC MOSFET cross-switch hybrid. *IEEE Electron Device Letters*, 2016, 37(9): 1178-1180.
- [73] K F Hoffmann, J P Karst. High frequency power switch - improved performance by MOSFETs and IGBTs connected in parallel. *2005 European Conference on Power Electronics and Applications*, Dresden, Germany, 11-14 Sept., 2005: 11-11. DOI: 10.1109/EPE.2005.219594.
- [74] K Ishikawa, S Yukutake, Y Kono, et al. Traction inverter that applies compact 3.3 kV/1200 A SiC hybrid module. *2014 International Power Electronics Conference*, Hiroshima, 2014: 2140-2144.
- [75] J San-Sebastian, A Rujas, L Mir, et al. Performance improvements using silicon carbide hybrid IGBT modules in traction application. *2016 International Conference on Electrical Systems for Aircraft, Railway, Ship Propulsion and Road Vehicles & International Transportation Electrification Conference*, Toulouse, 2016: 1-6.
- [76] T Takaku, H Wang, N Matsuda, et al. Development of 1700 V hybrid module with Si-IGBT and SiC-SBD for high efficiency AC690V application. *2015 9th International Conference on Power Electronics and ECCE Asia*, Seoul, 2015: 844-849.
- [77] H Wang, O Ikawa, S Miyashita, et al. 1700 V Si-IGBT and SiC-SBD hybrid module for AC690V inverter system. in Proc. *2014 International Power Electronics Conference*, Hiroshima, 2014: 3702-3706.
- [78] D Xiang, S Chen, H Wang, et al. 1700 V Si-IGBT and SiC-SBD hybrid module for AC690V inverter system. *2014 International Power Electronics and Application Conference and Exposition*, Shanghai, China, 2014: 93-97.
- [79] X Li, Z Zeng, H Chen, et al. Comparative evaluations and failure modes of wire-bonding packaged SiC, Si, and hybrid power modules. *2018 1st Workshop on Wide Bandgap Power Devices and Applications in Asia*, Xi'an, China, 2018: 16-22.
- [80] J Liu, W Su, X Tai, et al. Development of an inverter using hybrid SiC power module for EV/HEV applications. *2016 19th International Conference on Electrical Machines and Systems*, Chiba, 2016: 1-5.
- [81] D Li, H Luo, Y Huang, et al. Hybrid 3.3 kV/450 A half-bridge IGBT power module with SiC Schottky barrier diodes. *IET Power Electron*, 2020, 13(3): 405-412.
- [82] P Ning, L Li, X Wen, et al. A hybrid Si IGBT and SiC MOSFET module development. *CES Transactions on Electrical Machines and Systems*, 2017, 1(4): 360-366.
- [83] P Ning, T Yuan, H Cao, et al. The development of 1200 V SiC hybrid switched power modules. *2019 IEEE International Workshop on Integrated Power Packaging*, Toulouse, France, 2019: 7-11.
- [84] H Cao, P Ning, T Yuan, et al. A 1200V/400A hybrid module with Si-IGBT and SiC-MOSFET development. *International Exhibition and Conference for Power Electronics, Intelligent Motion, Renewable Energy and Energy Management*, Shanghai, China, 2019: 1-5.
- [85] P Ning, T Yuan, H Cao, et al. The development of a 1200V/400A SiC Hybrid Module. *2019 31st International Symposium on Power Semiconductor Devices and ICs*, Shanghai, China, 2019: 247-250.
- [86] J Lu, L Zhu, G Liu, et al. Device and system-level transient analysis in a modular designed sub-MW EV fast charging station using hybrid GaN HEMTs + Si MOSFETs. *IEEE Journal of Emerging and Selected Topics in Power Electronics*, 2019, 7(1): 143-156.
- [87] C Li, R Lu, C Li, et al. Space vector modulation for SiC and Si hybrid ANPC converter in medium-voltage high-speed drive system. *IEEE Transactions on Power Electronics*, 2020, 35(4): 3390-3401.
- [88] Z Quan, Y W Li. Multilevel voltage-source converter topologies with internal parallel modularity. *IEEE Transactions on Industry Applications*, 2020, 56(1): 378-389.
- [89] L Zhang, X Lou, C Li, et al. Evaluation of different SiC/Si hybrid three-level active NPC inverters for high power density. *IEEE Transactions on Power Electronics*, 2020, 35(8): 8224-8236.
- [90] Z Feng, X Zhang, S Yu, et al. Comparative study of 2SiC&4Si hybrid configuration schemes in ANPC inverter. *IEEE Access*, 2020, 8(1): 33934-33943.
- [91] J He, D Zhang, D Pan. An improved PWM strategy for "SiC+Si" three-level active neutral point clamped converter in high-power high-frequency applications. *2018 IEEE Energy Conversion Congress and Exposition*, Portland, OR, 2018: 5235-5241.

- [92] Y Jiao, F C Lee. New modulation scheme for three-level active neutral-point-clamped converter with loss and stress reduction. *IEEE Transactions on Industrial Electronics*, 2015, 62(9): 5468-5479.
- [93] Y Deng, J Li, K H Shin, et al. Improved modulation scheme for loss balancing of three-level active NPC converters. *IEEE Transactions on Power Electronics*, 2017, 32(4): 2521-2532.
- [94] G Zhang, Y Yang, F Iannuzzo, et al. Loss distribution analysis of three-level active neutral-point-clamped (3L-ANPC) converter with different PWM strategies. *2016 IEEE 2nd Annual Southern Power Electronics Conference*, Auckland, 2016: 1-6.
- [95] B Zhang, Q Ge, P Wang, et al. A novel modulation strategy providing loss balancing and neutral point potential balancing for three-level active neutral-point-clamped converter. *2015 17th European Conference on Power Electronics and Applications*, Geneva, 2015: 1-9.
- [96] D Pan, D Zhang, C Immer, et al. Pump-back validation of a medium voltage high-frequency “SiC+Si” hybrid three-level ANPC inverter for hybrid-electric propulsion application. *2019 IEEE International Electric Machines & Drives Conference*, San Diego, CA, USA, 2019: 1647-1654.
- [97] D Zhang, J He, D Pan. A megawatt-scale medium-voltage high-efficiency high power density “SiC+Si” hybrid three-level ANPC inverter for Aircraft hybrid-electric propulsion systems. *IEEE Transactions on Industry Applications*, 2019, 55(6): 5971-5980.
- [98] Y Zhang, J He, S Padmanaban, et al. Transistor-clamped multilevel H-bridge inverter in Si and SiC hybrid configuration for high-efficiency photovoltaic applications. *2018 IEEE Energy Conversion Congress and Exposition*, Portland, OR, 2018: 2536-2542.
- [99] L Zhang, Z Zheng, C Li, et al. A SiC/Si hybrid five-level active NPC inverter with improved modulation scheme. *IEEE Transactions on Power Electronics*, 2020, 35(5): 4835-4846.
- [100] L Huber, Y Jang, M M Jovanovic. Performance evaluation of bridgeless PFC boost rectifiers. *IEEE Transactions on Power Electronics*, 2008, 23(3): 1381-1390.
- [102] L Zhou, Y Wu, J Honea, et al. High-efficiency true bridgeless totem pole PFC based on GaN HEMT: Design challenges and cost-effective solution. *Proceedings of PCIM Europe 2015; International Exhibition and Conference for Power Electronics, Intelligent Motion, Renewable Energy and Energy Management*, Nuremberg, Germany, 2015: 1-8.
- [102] X Huang, Q Li, Z Liu, et al. Analytical loss model of high voltage GaN HEMT in cascode configuration. *IEEE Transactions on Power Electronics*, 2014, 29(5): 2208-2219.
- [103] Z Liu, Z Huang, F C Lee, et al. Operation analysis of digital control based MHz totem-pole PFC with GaN device. *2015 IEEE 3rd Workshop on Wide Bandgap Power Devices and Applications*, Blacksburg, VA, 2015: 281-286.
- [104] Q Li, B Liu, S Duan. Simplified analytical model for estimation of switching loss of cascode GaN HEMTs in totem-pole PFC converters. *Chinese Journal of Electrical Engineering*, 2019, 5(3): 1-9.
- [105] Z Huang, Z Liu, Q Li, et al. Microcontroller-based MHz totem-pole PFC with critical mode control. *2016 IEEE Energy Conversion Congress and Exposition*, Milwaukee, WI, 2016: 1-8.
- [106] C Li, Q Guan, J Lei, et al. An SiC MOSFET and Si diode hybrid three-phase high-power three-level rectifier. *IEEE Transactions on Power Electronics*, 2019, 34(7): 6076-6087.
- [107] O Kwon, J Kwon, B Kwon. Highly efficient single-phase three-level three-leg converter using SiC MOSFETS for AC-AC applications. *IEEE Transactions on Industrial Electronics*, 2018, 65(9): 7015-7024.



Li Zhang (S'11-M'13-SM'19) received the B.E. and Ph.D. degrees in electrical engineering from Nanjing University of Aeronautics and Astronautics (NUAA), Nanjing, China, in 2007 and 2012, respectively.

He joined the Faculty of Electrical Engineering, Hohai University, Nanjing, China, in 2014, where he is currently a professor. From October 2012 to September 2014, he was a post-doctoral research fellow with the Department of Electrical Engineering, Tsinghua University, Beijing, China. From July to August 2012, he was a visiting scholar of electrical engineering at the Department of Energy Technology, Aalborg University, Denmark. From October 2016 to October 2017, he was a visiting scholar of electrical engineering at the Department of Electrical and Computer Engineering, Ryerson University, Canada. He has authored and coauthored more than 60 peer-reviewed papers published in journals and conference proceedings. He is the holder of more than 20 patents. His current research interests include high-performance power converters and distributed generation technology.

Dr. Zhang was the recipient of the Outstanding Reviewer Award of *IEEE Transactions on Power Electronics* in 2014. He is currently an associate editor of the *Journal of Power Electronics*.



Zhongshu Zheng (S'18) was born in Shandong, China, in 1996. He received the B.S. degree in electrical engineering from Shandong Agricultural University, Taian, China, in 2018. He is currently working toward the Ph.D. degree in electrical engineering in Hohai University, Nanjing, China. His research interests include

DC-AC converter control, topology, and renewable energy generation technologies.



Xiutao Lou was born in Anhui, China, in 1996. He received the B.S. degree from the College of Energy and Electrical Engineering, Hohai University, Nanjing, China, in 2019, where he is currently working toward the M.S. degree in electrical engineering. His research interests include DC-AC converter control and power

electronics used in renewable energy generation.